Published in final edited form as:
Nat Neurosci. 2018 May ; 21(5): 725–735. doi:10.1038/s41593-018-0129-x.

Locomotor activity modulates associative learning in mouse cerebellum

Catarina Albergaria, **N. Tatiana Silva**, **Dominique Pritchett**, and **Megan R. Carey***
Champalimaud Neuroscience Programme, Champalimaud Centre for the Unknown, Lisbon, Portugal

Abstract

Changes in behavioral state can profoundly influence brain function. Here we show that behavioral state modulates performance in delay eyeblink conditioning, a cerebellum-dependent form of associative learning. Increased locomotor speed in head-fixed mice drove earlier onset of learning and trial-by-trial enhancement of learned responses that were dissociable from changes in arousal and independent of sensory modality. Eyelid responses evoked by optogenetic stimulation of mossy fiber inputs to the cerebellum, but not at sites downstream, were positively modulated by ongoing locomotion. Substituting prolonged, low-intensity optogenetic mossy fiber stimulation for locomotion was sufficient to enhance conditioned responses. Our results suggest that locomotor activity modulates delay eyeblink conditioning through increased activation of the mossy fiber pathway within the cerebellum. Taken together, these results provide evidence for a novel role for behavioral state modulation in associative learning and suggest a potential mechanism through which engaging in movement can improve an individual's ability to learn.

Introduction

Changes in behavioral state are associated with modulation of sensory processing in mice. Recent studies have shown that locomotor activity and arousal influence both spontaneous activity and sensory-evoked responses across mouse sensory cortices1–8, with important consequences for sensory perception. To what extent behavioral state modulation generalizes to other brain functions, however, remains unclear. Moreover, although locomotion also modulates activity within the cerebellar cortex9–12, the consequences of this modulation for

***Correspondence**: Megan R. Carey, PhD, Champalimaud Neuroscience Program, Av. Brasília, Doca de Pedrouços, 1400-038 Lisbon, Portugal, megan.carey@neuro.fchampalimaud.org.

Data availability
The data that support the findings of this study are available from the corresponding author upon reasonable request.

Code availability
Custom code is available from the corresponding author upon reasonable request.

Author contributions
CA and MRC designed the research plan. CA and NTS performed all experiments. CA and DP performed electrophysiological recordings. DP analyzed electrophysiology data. CA analyzed all data and prepared figures. CA and MRC wrote the manuscript.

Competing interests
The authors declare no competing financial interests.

Europe PMC Funders Author Manuscripts

cerebellar processing are largely unknown. Here we investigated the effects of behavioral state, and specifically locomotor activity, on delay eyeblink conditioning, a cerebellum-dependent form of associative learning.

In delay eyeblink conditioning, animals learn to close their eye in response to an initially neutral conditioned stimulus (CS) that is reliably predictive of an aversive unconditioned stimulus (US), such as a puff of air to the eye13–15. CS and US signals are conveyed to the cerebellum via distinct input pathways, mossy fibers (CS) and climbing fibers (US)16, each of which project to both the cerebellar cortex and deep cerebellar nucleus, where learning is thought to take place13,16,17.

We find that locomotor activity improves associative learning through mechanisms that are dissociable from arousal and independent of the modulation of cortical sensory responses. Further, optogenetic circuit dissection suggests that locomotion modulates delay eyeblink conditioning through mechanisms acting on the mossy fiber (CS) pathway within the cerebellum.

Results

We used a head-fixed apparatus with a freely rotating running wheel (Fig. 1A) to train mice in delay eyelid conditioning, a cerebellum-dependent form of associative learning18,19. Daily conditioning sessions included 100 trials in which a neutral conditioned stimulus (CS, unless otherwise indicated, a white LED) was paired with an air-puff unconditioned stimulus (US; a 50ms, 40psi air-puff directed at the eye). The CS preceded the US by 300ms and the two stimuli co-terminated (Fig. 1B). Eyelid closures were recorded with a high-speed (900 fps) video camera and conditioned (CR) and unconditioned response (UR) amplitudes were extracted with offline image processing (Fig. 1B). We measured the mouse's running continuously with an infrared sensor placed underneath the wheel (Fig. 1C).

Locomotor activity is associated with enhanced learning across mice

All mice trained with a light CS (N= 34) learned to reliably make well timed conditioned responses (CRs), steadily increasing both the percentage of trials that yielded CRs and their amplitude over the course of the daily training sessions (Fig. 1B,D). However, the rate of learning was variable across individuals (Fig. 1D).

How much each animal ran on average across the 20 training sessions was also highly variable (Fig. 1C). Comparing acquisition curves between the mice that ran the most and those that ran the least revealed that on average, more active animals acquired conditioned responses earlier (Fig. 1D). For each animal, we subdivided the acquisition of CRs into three phases (Supp. Fig. 1) and analyzed: the onset session of learning (Fig. 1E), the slope of the acquisition curve (Supp. Fig. 1B), and the plateau value of CR amplitude (Supp. Fig. 1C). All of these features were positively correlated with the animals' average running speeds, indicating that the more an animal ran on average, the earlier (Fig. 1E, onset value: slope=-34.4, $p < 0.001$), faster (Supp. Fig. 1B, slope of sigmoid: slope=4.5, $p < 0.01$) and better (Supp. Fig. 1C, plateau value: slope=0.8, $p < 0.05$) it learned.

Conditioned response amplitudes correlate with locomotor activity across sessions and trials

Even in mice that reach high levels of performance, there is variation in conditioned response amplitudes from session to session. We found that fluctuations in CR amplitudes from one session to the next were positively correlated with changes in the amount of locomotor activity (Fig. 1F: one-way ANOVA on random slope and intercepts linear mixed effects model (LME), $F(1,155)=24.271$, $p < 0.0001$). Thus, learning is correlated with locomotor activity not just across animals, but also across sessions.

There is also considerable trial-to-trial variation in the amplitude of conditioned responses within individual sessions, particularly before learning has saturated (Fig. 1G,H). To determine whether this variation was correlated with trial-to-trial changes in locomotor activity, we sorted trials by running speed and averaged their conditioned response amplitudes. There was a linear positive relationship (one-way ANOVA on LME, $F(1,180.29)=83.023$, $p < 0.0001$) between running speed and conditioned response amplitude (Fig. 1H), indicating that locomotor activity and eyelid conditioning performance are correlated on a trial-by-trial basis.

We next asked whether the locomotor enhancement of CRs was specific to learned, conditioned responses, or if eyelid closures were generally affected, by analyzing the blinks (unconditioned responses, URs) that the animal made in response to the unconditioned air-puff stimulus. We found that unconditioned response magnitudes were in fact negatively (one-way ANOVA on LME, $F(1,91.898)=27.366$, $p < 0.0001$), not positively, modulated by locomotor speed (Fig. 1I). This indicates that locomotor enhancement is specific to conditioned responses, and further suggests that increased salience of the unconditioned response, for example through stronger climbing fiber input, does not account for the improved learning.

Taken together, these results indicate that the positive correlation between locomotor activity and eyelid conditioning performance holds true across animals, sessions and trials.

Externally controlled changes in running speed are sufficient to modulate learning

When mice are free to initiate locomotor activity voluntarily, they run more during periods of high arousal8. To ask whether the enhanced learning performance observed in Fig. 1 was driven indirectly by these changes in arousal, or by locomotor activity itself, we used a motorized treadmill to control running speed. We trained two randomly assigned groups of mice to a light CS at different fixed speeds, 0.12m/s (N=5) or 0.18m/s (N=7), for the entire duration of each of the conditioning sessions. Mice were first habituated to the motorized wheel until they walked normally and displayed no external signs of distress at the assigned speed (Supp. Video 1).

Learning was faster and less variable on a fixed-speed motorized treadmill than on the freely-rotating, self-paced treadmill (Fig. 2A,B). Acquisition rate and conditioned response amplitudes were also running speed-dependent. Animals running at a faster speed learned earlier (Fig. 2A,B; $p < 0.0001$) and had larger CR amplitudes (Fig. 2C,D; $p < 0.01$) than mice on the slower treadmill. Interestingly, variability in learning was reduced on the

motorized treadmill, likely due to the elimination of variability in running within and across sessions.

The finding that externally imposed changes in running speed are sufficient to modulate learning extends the correlative data from the self-paced treadmill to provide causal evidence that increases in locomotor activity enhance learning.

Modulation is CS-modality independent and dissociable from changes in arousal

Behavioral state differentially affects cortical processing of sensory stimuli of different modalities in mice2,4,5,8,20,21. In particular, increased locomotion is associated with positive modulation of visual responses2,3, but negatively modulates responses to auditory stimuli4,5. To test whether the correlation we observed between locomotor activity and learning performance could be specific to the visual conditioned stimulus, we repeated the experiments from Fig. 1 but replaced the visual CS with either a tone or a vibratory stimulus delivered to the whisker (Fig. 3A). As was the case with a visual CS, we found that for both auditory and tactile CS modalities, increased locomotor activity on a self-paced treadmill was a positive predictor of larger CR amplitude from trial-to-trial (Fig. 3B; one-way ANOVA on LME, whisker CS: $F(1,159.8)=11.499$, $p < 0.001$) and tone CS: $F(1,85.5)=32.255$, $p < 0.0001$). Inspecting acquisition curves revealed that learning to a whisker CS (N=25) proceeded marginally significantly faster in mice that ran more rather than less (Fig. 3C, slope=-15.7, p=0.052). For the tone CS (N=16), we observed a similar, though not statistically significant, trend (Fig. 3C; slope=-8.9; p=0.49).

We next took advantage of the reduction in variability on the motorized treadmill (Fig. 2), to ask whether changes in running speed are sufficient to modulate acquisition of learning to a non-visual CS modality. We trained two groups of mice to a whisker CS at different fixed treadmill speeds, 0.12m/s (N= 5) or 0.18m/s (N=6). As previously seen using a visual CS (Fig. 2A), the rate of learning to a whisker CS was speed-dependent (Fig. 3D,E, $p < 0.001$). There was a corresponding enhancement of CR amplitude on the fast vs. slow treadmill (Fig. 3F,G; $p < 0.01$).

The previously described modulation of cortical sensory responses in mice is thought to result in part from changes in arousal, as measured by pupil size22,23, rather than locomotor activity *per se*1,21,22,24,25. Using a non-visual conditioned stimulus allowed us to measure pupil diameter to dissociate the effects of arousal vs. locomotor activity on trial-to-trial modulation of eyeblink conditioning. As has been previously shown1,8, we found that on average, locomotor activity and pupil size were positively correlated with each other on a self-paced treadmill (Supp. Fig. 2A). However, we found no trial-to-trial correlation between pupil size and conditioned response amplitudes (Supp. Fig. 2B; one-way ANOVA on LME, whisker CS: $F(1,225)=0.203$, $p=0.65$; tone CS: $F(1,162)=0.1736$, $p=0.68$). These results suggest, surprisingly, that trial-to-trial CR amplitude is positively modulated by locomotor activity but not arousal, despite the average correlation between those two signals.

We further investigated the intricate relationship between CR amplitude, running speed and arousal by separately analyzing trials consisting of low and high levels of locomotor activity and pupil size (Supp. Fig. 2C-F). We found that for both CS modalities (tactile and

auditory), and for both low and high levels of arousal, CR amplitudes were positively modulated by speed (Supp. Fig. 2C,D). In contrast, there was no positive correlation between arousal and CR amplitude for either whisker (Supp. Fig. 2E) or auditory (Supp. Fig. 2F) CS's. In fact, at low speeds CR amplitudes were significantly *negatively* modulated by increased arousal for both CS modalities (Supp. Fig. 2E,F). Further, on trials in which the mice were still, CR amplitude was *negatively* correlated with pupil size for both whisker (Supp. Fig. 2G, green) and auditory (Supp. Fig. 2G, red) CS's.

We next took advantage of the ability to hold locomotor speeds constant on the motorized treadmill in order to isolate the correlation between conditioned response amplitudes and pupil size. Importantly, there was no difference in average pupil size at the two motorized speeds (Fig. 3H, inset). This suggests that while arousal (as measured by pupil size) clearly influences locomotor activity, the reverse is not necessarily true. Consistent with the data from the self-paced treadmill (Supp. Fig. 2E,F), increased arousal on the motorized treadmill was not associated with larger CRs to a whisker CS (Fig. 3H, one-way ANOVA on LME, slow speed: N=5, $F(1,38)=2.929$, $p=0.095$), and in fact, for faster motorized speeds, there was a negative correlation between pupil size and CR amplitude (one-way ANOVA on LME, fast speed: N=6, $F(1,102)=10.35$, $p < 0.01$).

In summary, across experimental conditions, locomotor activity is associated with faster learning and larger conditioned responses regardless of the sensory modality of the CS, and this effect can be dissociated from the sometimes competing effects of arousal.

Learning to an optogenetic conditioned stimulus is positively modulated by locomotor activity

The finding that locomotor activity positively modulated conditioned responses regardless of CS modality (Fig. 3) suggested to us that it might act downstream of CS processing, in eyelid conditioning areas themselves. In delay eyelid conditioning, the CS is conveyed to the cerebellum via mossy fiber inputs, and electrical stimulation of MFs has been shown to substitute for a sensory CS to drive eyelid conditioning in rabbits26. We reasoned that if locomotor modulation of eyeblink conditioning occurred downstream of mossy fiber inputs to the cerebellum, then learning to a CS consisting of direct mossy fiber stimulation should be enhanced by locomotor activity.

To test this hypothesis, we implanted fiber optics into an eyelid region of the cerebellar cortex (Supp. Fig. 3A) of Thy1-ChR2/EYFP transgenic mice expressing channelrhodopsin 2 (ChR2) in cerebellar mossy fibers (from here on termed MF-ChR2 mice). Consistent with previous studies27, we verified that mossy fiber afferents to both cerebellar cortex and AIP expressed ChR2-YFP in these mice (Supp. Fig. 3A,D; Supp. Fig. 4A).

We first asked whether optogenetic stimulation of MF terminals within the cerebellar cortex could act as a conditioned stimulus for eyeblink conditioning (Fig. 4A,B). For these experiments we used low-power laser stimulation (0.25 to 0.9 mW), well below the threshold for evoking eyelid closures in naïve animals, as a CS (see early trials in Fig. 4C). As with a sensory CS, mice gradually learned to make well-timed eyelid closures in response to optogenetic stimulation of cortical MFs (Fig. 4C). On a self-paced treadmill,

animals acquired CRs at rates that were, overall, comparable to those conditioned with a sensory CS (Fig. 4D, blue filled circles, N=7). However, given that these particular mice exhibited low levels of spontaneous locomotor activity, their acquisition was faster than would have been expected based on the relationship between locomotion and learning onset we described in Figs. 1 and 2 (Fig. 4E), perhaps due to bypassing noise in sensory processing of the CS28.

We next asked whether animals would acquire conditioned responses to a cortical MF-optogenetic CS even faster if they were running on a motorized treadmill. Because learning was already quite rapid, we were surprised to find that running on a fast motorized treadmill accelerated the onset of learning to a mossy fiber conditioned stimulus (Fig. 4 D,E: fast motorized (N=7) vs. self-paced (N=7), fitted with linear regression: slope=-16.8; $p < 0.001$).

To determine whether locomotor activity modulated the expression of learning to an optogenetic CS, animals (N=15) were placed on the motorized wheel for post-conditioning test sessions with 50% CS+US and 50% CS-only trials. Each animal was tested at two speeds (0.06m/s and 0.18m/s; trials were presented in speed blocks and the order of blocks was counterbalanced across animals) (Fig. 4F,G). CR amplitudes were larger when the animals were running at faster speeds (Fig. 4F,G: $p < 0.01$). Finally, as was the case with sensory CS's, the locomotor modulation of optogenetically-evoked CRs could not be accounted for by changes in arousal, as CRs were either not significantly correlated (at the faster speed) or *negatively* correlated (at the slower speed) with pupil size (Fig. 4H, one-way ANOVA on LME, fast speed: $F(1,55.3)=0.845$, $p=0.36$; slow speed: $F(1,11.9)=59.5$, $p=0.001$).

Thus, locomotor activity improves acquisition and expression of learning to an optogenetic mossy fiber CS, suggesting that locomotor activity acts downstream of cerebellar mossy fibers to modulate delay eyeblink conditioning.

Locomotor activity modulates eyelid closures within the cerebellum

Mossy fibers synapse onto granule cells in the cerebellar cortex. Granule cell axons, the parallel fibers, project to Purkinje cells, which in turn inhibit deep nucleus neurons, converging once again with the direct mossy fiber-to-deep nucleus inputs (Fig. 5A). Higher intensities of optogenetic manipulation of both mossy fibers and neurons downstream within the cerebellar circuit have been shown to drive eyelid closures in mice29.

We next asked whether eyelid closures elicited by optogenetic stimulation of different circuit elements within the cerebellum could be modulated by locomotor activity. To this end, we examined eyelid closures evoked by optogenetic stimulation at different sites in mouse lines with differential ChR2 expression patterns, and compared and contrasted the observed modulation by locomotor activity.

As expected, optogenetic stimulation in the eyelid region of cerebellar cortex (Supp. Fig. 3A) or the anterior interpositus deep cerebellar nucleus (AIP, Supp. Fig. 3D) of MF-ChR2 mice evoked increases in multiunit neural activity (Fig. 5F,G) and short-latency, stimulation-intensity dependent eyelid closures (Fig. 5B,C). Moreover, optogenetic stimulation in the

cerebellar cortex of mice expressing ChR2 specifically in Purkinje cells (Pkj-ChR2; Supp. Fig. 3C, Supp. Fig. 4C) yielded increases in Purkinje cell activity (Fig. 5H), and resulted in stimulation-intensity dependent eyelid closures at laser *offset* (Fig. 5D).

Comparing the relative effects of locomotor activity on eyelid closures evoked by optogenetic stimulation at these different sites and mouse lines revealed differential effects. On a self-paced treadmill, eyelid closures evoked by optogenetic stimulation within the cerebellar cortex of MF-ChR2 mice (MF-ChR2-ctx) were larger on trials in which mice were running faster (Fig. 5J, blue, N=8, one-way ANOVA on LME, $F(1,1068.8)=5.01$, $p < 0.05$). The same pattern of dependence on locomotor activity was observed in mice running on a motorized treadmill (Fig. 5K; $p < 0.05$ for fast (0.18 m/s) vs. slow (0.06 m/s) motorized treadmill, N=7). Interestingly, this effect was highly location specific. In the same mouse line, optogenetic stimulation in the AIP (MF-ChR2-AIP) evoked eyelid closures that were negatively correlated with locomotor speed on the self-paced (Fig. 5J, cyan, $F(1,501.8)=4.02$, $p < 0.05$, N=5) and motorized treadmills (Fig. 5L, N=6, $p < 0.05$). Unlike the MF-ChR2 mice, however, the eyelid closures elicited by optogenetic stimulation within the cerebellar cortex of Pkj-ChR2 mice were not modulated by locomotor activity (Fig. 5M,N=10, $p=0.94$). Taken together, these results are consistent with the idea that the cerebellar cortex, somewhere between mossy fibers and Purkinje cells, is a site of action for the observed effects of locomotion on conditioned eyelid closures.

Next, we analyzed optogenetically-evoked eyelid closures in mice in which ChR2 expression was targeted to cerebellar granule cells (gc-ChR2 mice, Supp. Fig. 3B; Supp. Fig. 4B). Optogenetic stimulation in gc-ChR2 mice also evoked intensity-dependent, short-latency eyelid closures and changes in multiunit activity (Fig. 5E,I), and were modulated by locomotor activity (Fig. 5N). However, again, unlike optogenetic stimulation in the cerebellar cortex of MF-ChR2 mice, these eyelid closures were negatively correlated with locomotor activity on both self-paced (Fig. 5J, green, $F(1,939.5)=30.68$, $p < 0.0001$, N=11) and motorized treadmills (Fig. 5N, $p < 0.05$, N=11).

We took several steps to ensure the spatial and cell-type specificity of these optogenetics experiments. We empirically verified the predicted effective spatial separation by placing a fiber in the AIP of gc-ChR2 mice (Supp. Fig. 5A). Even at relatively high laser intensities, this stimulation failed to drive blinks (Supp. Fig. 5B, grey), in contrast to fiber placement within the cortex of the same mice (Supp. Fig. 5B, green; Fig. 5E). Second, we observed clear differences in fluorescence expression patterns upon histological examination of each mouse line, which in every case were consistent with previous descriptions of cell-type specificity (Supp. Fig. 4). Third, at the same site within the cerebellar cortex, optogenetic stimulation in MF-ChR2 and gc-ChR2 evoked eyelid closures at stimulation *onset*, while stimulation in Pkj-ChR2 mice evoked responses solely at stimulus *offset* (Fig. 5 B-E). These differential responses are as predicted based on previous studies, and are consistent with the sign inversion introduced by inhibitory interneurons between granule cells and Purkinje cells. In addition, the same photostimulation protocol applied in non-ChR2 expressing, wildtype animals did not elicit eyelid movement (Supp. Fig. 5C). Finally, while histological examination of gc-ChR2 mice was consistent with specific ChR2-YFP expression in granule cells within the cerebellar cortex (Supp. Fig. 3B, Supp. Fig. 4B), and we obtained

electrophysiological (Fig. 5I) and behavioral (Supp. Fig. 5B) responses consistent with this finding, we cannot entirely rule out the possibility of some additional ChR2 expression in non-granule cells in the gc-ChR2 mice. Importantly, however, additional non-specific ChR2 expression in any other cells in the cerebellar cortex of the gc-ChR2 mice (or similarly, in MF-ChR2 or Pkj-ChR2 mice) would also be downstream of MFs and upstream of Purkinje cells, i.e., still within the cerebellar cortex.

Optogenetic ‘tickling’ of cerebellar mossy fibers is sufficient to enhance conditioned responses

Recent studies demonstrating enhancement of MF-gc synaptic transmission via glutamate spillover during locomotion10, as well as multimodal convergence of mossy fiber inputs onto single granule cells30–32 present a potential mechanism for our findings. Specifically, elevation in mossy fiber tone during locomotion could enhance the representation of the CS at the level of individual granule cells, which must sum activity over multiple MF inputs to reach spike threshold33, and this enhancement could be responsible for the improved learning and expression of eyeblink conditioning during locomotion (Fig. 6A).

To explore this possibility, we used prolonged, low-intensity optogenetic stimulation of mossy fibers in MF-ChR2 mice (Fig. 6B) and asked whether this stimulation could substitute for increased mossy fiber activity during locomotion and enhance conditioned responses to a visual CS.

We placed an optical fiber in the eyelid region of cerebellar cortex, as in the previous experiments, and reduced the stimulation intensity even further below the levels used in Fig. 4. Electrophysiological recordings verified the efficacy of this prolonged, low-intensity optogenetic stimulation (Fig. 6C). Blocks of trials with this low-level background stimulation (‘tickle’ blocks) were alternated with blocks without any stimulation (‘no tickle’ blocks), while presenting a visual CS paired with an airpuff US and holding locomotor speed constant (at 0.12m/s) (Fig. 6B). All animals showed increased CR amplitudes in blocks of trials with stimulation vs. blocks without stimulation (Fig. 6D,E: N=6, $p < 0.01$). Identical experiments conducted in non-ChR2 expressing wildtype animals to control for nonspecific effects of photostimulation had no effect on CR amplitudes (Fig. 6E, black).

These results demonstrate that prolonged, low intensity stimulation of mossy fibers is sufficient to enhance conditioned responses, even in the absence of changes in arousal.

Discussion

We found that delay eyeblink conditioning in mice is modulated by both volitional and externally-imposed locomotor activity. Acquisition and expression of learning were enhanced in a speed-dependent manner. The effects of locomotor activity generalized across CS modalities, were specific to learned responses, and were dissociable from changes in arousal. Optogenetic activation of cerebellar input pathways and circuit sites downstream provided evidence that locomotor activity acts within the cerebellum to modulate learning. Our findings indicate a novel role for behavioral state in the modulation of associative

learning and suggest a potential mechanism through which engaging in motor activities may improve an individual's ability to learn.

Locomotor activity modulates delay eyeblink conditioning

Several previous studies have highlighted the difficulties in establishing robust eyeblink conditioning in head-fixed mice34,35. Performance improved when mice were allowed to run freely on a running wheel, an observation that has been attributed to removing stress and allowing the animals to engage in one of their favorite activities36. Our finding that locomotor activity modulates delay eyelid conditioning directly, within the cerebellum, provides a possible alternative mechanism to account for the earlier difficulties and the success of more recent approaches.

Locomotor activity enhanced several features of learning. The onset and rate of learning were modulated in a speed-dependent way when animals were running on both self-paced and motorized treadmills. Remarkably, holding running speed constant with a motorized treadmill virtually eliminated the substantial animal-to-animal variability in acquisition that was observed on a self-paced treadmill (Fig. 2). Expression of learning, as measured by trial-to-trial or session-to-session fluctuations of CR amplitude, was also positively modulated by locomotion (Figs. 1, 3,4).

Dissociable effects of locomotion and arousal

Several lines of evidence in our data suggest that the positive correlation between locomotor activity and learning is dissociable from the effects of arousal, as measured by pupil size1,21. First, while self-paced running speed is influenced by arousal, in the case of the motorized treadmill, the speed was externally imposed, and there was no difference in average pupil sizes at different motorized treadmill speeds (Fig. 3H). Nevertheless, responses were locomotor speed-dependent on both self-paced and motorized treadmills, across all sensory and optogenetic conditioned stimuli. Second, not only did we never observe a positive modulation of CR's by arousal, interestingly, we observed negative modulation of eyelid closures by arousal across a broad range of stimulus conditions, including all sensory modalities (Supp. Fig. 2E,F; Fig. 3H), optogenetic stimulation (Fig. 4H), and even unconditioned responses (Fig. 1I). Thus, it seems probable that there is a generalized arousal-based suppression within the eyelid closure pathway (likely downstream of mossy fibers/AIP), that is overshadowed in most of our experiments by the more specific enhancement of CR's by locomotor activity.

One mechanistic possibility is that neuromodulator release related to locomotor activity positively modulates the effectiveness of MF-gc transmission by affecting some combination of mossy fiber terminals, granule cells, or Golgi cells. The cerebellum receives many neuromodulatory inputs, in particular, noradrenergic signals relating to arousal23,37 that are known to affect cerebellar circuit activity in a variety of ways38–42. However, the ability to clearly dissociate the effects of locomotor activity *per se* from changes in pupil size (Fig. 3H, Supp. Fig. 2) makes it unlikely that the effects we describe here can be explained by a simple relationship between noradrenergic activation and performance23,24,43. It is still possible that other locomotor-related neuromodulatory signals are involved. However, the

Europe PMC Funders Author Manuscripts

results of the ‘tickle’ experiment in Fig. 6 suggest that it may not be necessary to invoke neuromodulatory mechanisms to explain the modulation of cerebellar circuit processing we describe here.

Mechanisms of locomotor modulation of learning

Several lines of evidence suggest that locomotor activity acts within the cerebellum to modulate eyeblink conditioning. First, modulation generalizes across CS modalities – responses to visual, auditory, and somatosensory CS’s were similarly enhanced by locomotion (Fig. 3). Second, learning to an optogenetic CS in the cerebellar cortex of mice expressing ChR2 in mossy fiber inputs was also positively modulated by locomotion (Fig. 4). This experiment bypassed sensory processing of the CS that occurs upstream of the cerebellum, thereby demonstrating that locomotor modulation occurs downstream of cerebellar mossy fibers.

Our results provide some clues about the sites where locomotor activity may exert its effects. We compared and contrasted the effects of optogenetic stimulation of the cerebellar cortex and deep nucleus of mice in which ChR2 was differentially targeted to distinct sets of cerebellar cell types. We found that blinks elicited by stimulation of mossy fibers in the cerebellar cortex, but not of Purkinje cells, granule cells, or in the AIP, were positively modulated by locomotor activity (Fig. 5). Given that optogenetic stimulation of neurons upstream, but not downstream, of the site of locomotor modulation would be predicted to evoke eyelid closures that would be positively modulated by locomotion, these findings are consistent with the idea that there is a site of locomotor modulation within the cerebellar cortex, downstream of mossy fibers, and upstream of Purkinje cells.

The strength of the conclusions that can be reached from these optogenetic circuit dissection experiments depends on the degree of spatial and cell-type specificity that can be achieved. Several lines of evidence support the specificity of these experiments. First, the MF-ChR2 and Pkj-ChR2 lines have been previously used and validated, and we obtained histological, electrophysiological, and behavioral results consistent with their previously-described, specific patterns of functional ChR2 expression (i.e., a blink at laser onset with mossy fiber stimulation, at laser offset with Purkinje cell stimulation, and no blink in non-ChR2 expressing controls, Fig. 5). Second, the failure to elicit a blink with a fiber placed in the AIP of gc-ChR2 mice (Supp. Fig. 5A,B) demonstrates that illumination was highly spatially specific, as predicted for the low stimulation intensities we used and the distance between the sites. Thus, while we cannot exclude the possibility that there may have been additional functional ChR2 expression in other cell types in some of these experiments, the totality of the data support the conclusion that there is a site of locomotor modulation within the cerebellar cortex that is sufficient to enhance behavioral responses.

We cannot completely rule out the existence of possible additional locomotor modulation within AIP. Some ChR2 expression in the cerebellar deep nuclei, including possibly nucleocortical reafferents29, could be present and mask modulation of MF inputs to AIP. In addition, MF-ChR2 stimulation in the cortex or AIP could have antidromically activated MF collaterals. However, the differential modulation observed at the two sites suggests that

inadvertent antidromic stimulation was not a major factor in these experiments, perhaps because of the morphology and long range nature of mossy fiber axons44–46.

In summary, of all of the combinations of ChR2 expression patterns and fiber placements that we tested, only eyelid closures elicited by stimulation within the cerebellar cortex of MF-ChR2 mice were positively modulated with locomotion. Thus, taken together, these findings suggest that locomotor activity acts within the cerebellar cortex, perhaps at the mossy fiber-granule cell connection, to enhance eyeblink conditioning.

An intriguing possibility is that convergence of locomotor and CS signals onto individual granule cells allows them to convey more reliable CS information to interneurons and Purkinje cells9,10,30,47–49. Granule cells receive input from 3-5 distinct mossy fibers, as well as inhibition from Golgi cells. Recent studies have demonstrated multimodal convergence of mossy fiber inputs onto single granule cells30–32,49. Granule cells require multiple simultaneous MF inputs to reach threshold33, and MF-gc synaptic transmission is enhanced by glutamate spillover during locomotion10. Convergence of locomotor and conditioned stimulus MF inputs to a granule cell would therefore be expected to increase the probability of a postsynaptic action potential in response to the CS during locomotion. Modulation of Golgi cell-granule cell inhibition during locomotion50 could also play a role.

Our last experiment (Fig. 6) revealed that elevated mossy fiber tone is sufficient to enhance conditioned responses to a visual CS, even in the absence of changes in arousal. These experiments suggest that locomotor activity modulates eyeblink conditioning through a mechanism that could allow not only locomotor signals, but any generalized increase in mossy fiber activity, to modulate cerebellar learning.

Conclusion

We found that locomotor activity acts within the cerebellum, on rapid time scales and independently of competing effects of arousal, to enhance associative learning. The modulation of associative learning by behavioral state that we describe here is distinct from the previously described modulation of sensory cortical processing, both in terms of where and how it acts. Together with previous work, these findings suggest that the relationship between behavioral state and motor output under natural conditions will ultimately depend on the complex interplay between arousal and locomotor signals and their varying actions across brain areas.

Methods

Animals

All procedures were carried out in accordance with the European Union Directive 86/609/EEC and approved by the Champalimaud Centre for the Unknown Ethics Committee and the Portuguese Direcção Geral de Veterinária (Ref. No. 0421/000/000/2015). All procedures were performed in male and female C57BL/6 mice approximately 10–14 weeks of age. The Thy1-ChR2/EYFP mouse line27,51 was obtained from The Jackson Laboratory (stock number: 007612). The Pkj-ChR2 mouse line was obtained by crossing L7-Cre mice

(stock number: 004146,52) with ChR2-EYFP-LoxP mice (stock number: 012569,53), both lines from The Jackson Laboratory. The gc-ChR2 mouse line was obtained by crossing Gabra6-Cre mice54, which we previously used to knock out cannabinoid CB1 receptors specifically from granule cells in cerebellar cortex55) with ChR2-EYFP-LoxP from The Jackson Laboratory (stock number: 012569)53. Mice were housed in groups of 3-5 with food and water *ad libitum* and were kept on a reverse light cycle (12:12 hour light/dark) so that all experiments were performed during the dark period while mice were more active.

Surgical procedures

In all our surgeries, animals were anesthetized with isoflurane (4% induction and 0.5 – 1% for maintenance), placed in a stereotaxic frame (David Kopf Instruments, Tujunga, CA) and a head plate was glued to the skull with dental cement (Super Bond – C&B).

For *in vivo* electrophysiological recordings, craniotomies were drilled over the eyelid area of cerebellar cortex56–60 (RC -5.7, ML +1.9) and then filled over with a silicon based elastomer (Kwik-cast, WPI) that was easily removed just before recording sessions. For optogenetic manipulations, optical fibers with 200μm core diameter, 0.22 NA (Doric lenses, Quebec, Canada) were lowered into the brain through smaller craniotomies, and positioned at the cortical eyelid region (RC -5.7, ML +1.9, DV 1.5) or just over the AIP (RC -6, ML +1.7, DV 2.1)61. The implants were fixed into place using dental cement (Super Bond – C&B). After any surgical procedure, mice were monitored and allowed ~1-2 days of recovery.

Behavioral procedures

The experimental setup was based on previous work62,63. For all behavioral experiments, mice were head-fixed but could walk freely on a Fast-Trac Activity Wheel (Bio-Serv) and habituated to the behavioral setup for at least 4 days prior to training. To externally control the speed of the treadmill, a DC motor with an encoder (Maxon) was used. For experiments on the motorized treadmill, mice were additionally habituated to walk at the target speed until they walked normally and displayed no external signs of distress (Supp. Video 1). There was no difference between the groups in the amount of time habituated. Externally imposed speeds were chosen empirically by observing the comfort range of the head-fixed mice on the motorized treadmill; they roughly correspond to slow overground walking speeds in head-free mice64. Slower speeds were used in Figs. 4 and 5 to match the slower walking preferences of the Thy1 mice.

Running speed was measured using an infra-red reflective sensor placed underneath the treadmill. Eyelid movements of the right eye were recorded using a high-speed monochromatic camera (Genie HM640, Dalsa) to monitor a 172 x 160 pixel region, at 900fps. Custom-written software using LabVIEW, together with a NI PCIE-8235 frame grabber and a NI-DAQmx board (National Instruments), was used to trigger and control all the hardware in a synchronized manner.

After habituation, most of the behavioral experiments consisted of 3 phases: acquisition, test and extinction. Acquisition sessions consisted of the presentation of 90% CS-US paired trials and 10% CS-only trials, which allow for the analysis of the kinematics of CRs without

the masking effect that comes from the US-elicited reflex blink. Test sessions were presented after mice had asymptote and consisted of 50% paired and 50% CS-only trials62. During extinction 100% of the trials presented were CS-only. Each session consisted of 110 trials, separated by a randomized inter trial interval (ITI) of 5-20s. In each trial, CS and US onsets were separated by a fixed interval (ISI) of 300ms and both stimuli co-terminated.

For all training experiments, the unconditioned stimulus (US) was an air-puff (30-50psi, 50ms) controlled by a Picospritzer (Parker) and delivered via a 27G needle positioned ~0.5cm away from the cornea of the right eye of the mouse. The direction of the air-puff was adjusted for each session of each mouse so that the unconditioned stimulus elicited a normal eye blink. The CS had a 350ms duration and was either a 1) white light LED positioned ~3cm directly in front of the mouse; 2) a piezoelectric device placed ~0.5cm away from the ipsilateral vibrissal pad; or 3) a tone (10kHz, 68dB) delivered by a speaker placed ~15cm away from the mouse.

Acquisition of eyeblink conditioning was conducted only once per animal; expression and acquisition data within individual figures comes from the same animals. Some animals from Fig. 5 were also used in Fig. 4.

Behavioral analysis

The video from each trial was analyzed offline with custom-written software using MATLAB (MathWorks). The distance between eyelids was calculated frame by frame by thresholding the grayscale image of the eye and extracting the count of pixels that constitute the minor axis of the elliptical shape that delineates the eye. Eyelid traces were normalized for each session, ranging from 1 (full blink) to 0 (eye fully open). Trials were classified as CRs if the eyelid closure reached at least 0.1 (in normalized pixel values) and occurred between 100ms after the time of CS onset and the onset of US. The average running for each animal was calculated by summing the average speed of each session (total distance run divided by session duration) and dividing by the total number of learning sessions, usually 20. Running speed for trial was calculated by dividing the distance run in the intertrial interval preceding the current trial by the elapsed time.

Optogenetic stimulation

Light from a 473 nm laser (LRS-0473-PFF-00800-03, Laserglow Technologies) was controlled with custom-written code using LabView software, and laser power was adjusted for each mouse and controlled for each experiment using a powermeter (Thorlabs) at the beginning and end of each session. To investigate the modulation of locomotion on laser-driven blinks (Fig. 5), the intensity of the laser was adjusted so that it would elicit an intermediate eyelid closure. For driving a blink via photostimulation of mice expressing ChR2 in mossy fibers (eyelid region of cerebellar cortex or AIP), Purkinje cells, or granule cells, 4ms pulses were delivered at 100Hz for 50ms. For the MF-ChR2 mice, laser powers ranged from 0.16-2 mW, which for the 100-micron radius optical fiber used in our study corresponds to laser intensities of 5 to 64 mW/mm2 (where laser intensity equals power divided by the cross-sectional area of the fiber). For the gc-ChR2 mice, laser powers ranged from 0.5-4 mW, corresponding to intensities of 16-127 mW/mm2. For the Pkj-ChR2 mice,

laser powers ranged from 2.5-15 mW, corresponding to intensities of 80-480 mW/mm2. Note that all of these values are very low compared to previous studies56,65. With these low intensities, stimulation is likely to be highly localized (predicted spread from cortex to AIP sites of <1% based on https://web.stanford.edu/group/dlab/optogenetics; verified in Supp. Fig. 5).

For activation of ChR2 in mossy fibers within the cerebellar cortex as a CS (Fig. 4), laser power was lowered below the threshold for detectable eyelid movement upon repeated stimulus presentation. The optogenetic CS consisted of stimulation of 350ms duration (2ms pulses delivered at 100Hz) and was paired with a co-terminating, 50ms airpuff US. Laser power ranged from 0.25 to 0.9 mW, corresponding to intensities (power output per unit area) of 8 to 30mW/mm2.

For low-level background stimulation of mossy fibers in the cerebellar cortex (Fig. 6), laser power ranged from 0.12 to 0.5 mW, corresponding to laser intensities (power per unit area) of 4 to 16mW/mm2. During ‘tickle’ blocks, 2ms pulses were delivered at 50Hz for the block duration. ‘Tickle’ blocks (10 trials) were alternated with no stimulation blocks.

Electrophysiological recordings

Single and multi-unit recordings were performed with quartz-insulated tungsten tetrodes (Thomas Recording, tip type A, impedances between 1-3 MOhm) or Tungsten microelectrodes (75 um shaft diameter, FHC) mounted on a 200um diameter optic fiber (fiber placed with 300um offset to minimize the opto-electric artifact). Electrodes were controlled using a 3-axis stereotaxic manipulator (Kopf) or a motorized 4-axis micromanipulator (PatchStar, Scientifica).

Recordings were performed with an Intan digital amplifier/headstage with the Open Ephys digital acquisition board66. Online monitoring was done using a custom Bonsai software interface67. All recordings were digitized from the wide-band signal (0.1 Hz - 10kHz, sampled at 30kHz), and sorted offline using custom Matlab code for unit analysis. Single units were determined by checking the unit parameters, e.g. ISI, firing rate, and LCV68.

In awake, head-fixed mice running on a treadmill, we targeted the eyeblink microzone either by monitoring the local field potential for a large depolarization to an air-puff stimulus applied to the ipsilateral eyelid61 or by optogenetic stimulation driving a blink response.

We recorded from a total of 56 recording sites, from 8 animals (6 Thy1-ChR2 animals, 4 sites in AIP and 24 sites in the cerebellar cortex, 1 Gabra6Cre-ChR2 mouse with 5 recording sites, and 1 L7-ChR2 mouse with 23 sites). Recording sites were chosen for clear unit activity. However, across all recording sites, even in the presence of a well-isolated single unit, spike waveform and ISI changes during laser stimulation indicated the presence of multi-unit activity to optogenetic manipulation.

Histology

After photostimulation experiments using chronically implanted optical fibers dipped in DiI (Sigma), animals were perfused transcardially with 4% paraformaldehyde and their brains

removed, so that fiber placement could be examined (Supp. Fig. 3). Coronal sections were cut in a vibratome and mounted on glass slides with mowiol mounting medium. Histology images were acquired with an upright confocal laser point-scanning microscope (Zeiss LSM 710), using a 10x or 40x objective.

Statistical analysis

All statistical analyses were performed using the Statistics toolbox in MATLAB. For the correlation between speed vs onset session (Fig. 1E; Fig. 3C; Fig. 4E) and speed vs slope or plateau (Supp. Fig. 1), we used linear regression analysis. For the correlation between delta speed vs delta CR amplitude from session-to-session (Fig. 1F), speed vs. CR amplitude (Fig. 1H; Fig. 3B; Supp. Fig. 2), and speed vs UR area (Fig. 1I), we used a mixed ANOVA on the averages from all animals. We used the same approach to compare the effects of speed and arousal (pupil) on CRs (Fig. 3H; Fig. 4H; Supp. Fig. 2). For the correlation of speed vs. laser-driven eyelid responses (Fig. 5J), we used a mixed ANOVA on all trials, adding animal as a random term. To compare the amplitudes of eyelid closure on the fast and slow speeds on the motorized treadmill (Fig. 4G; Fig. 5K,L,M,N;), and also with and without low-level background stimulation of mossy fibers (Fig. 6E), we used a Student's paired t-test. To test effects on onset of learning (Fig. 2B; Fig. 3E) and average CR amplitude (Fig. 2D; Fig. 3G) at fast vs. slow speeds on the motorized treadmill, we used a two-sample t-test. All t-tests were two-sided. Differences were considered significant at $*p < 0.05$, $**p < 0.01$ and $***p < 0.001$. No statistical methods were used to pre-determine sample sizes but our sample sizes are similar to those reported in previous publications56,63. Unless otherwise indicated, data distribution was assumed to be normal. Data collection and analysis were not performed blind to the conditions of the experiments; mice were randomly assigned to specific experimental group without bias and no animals were excluded. A Life Sciences Reporting Summary is available.

Supplementary Material

Refer to Web version on PubMed Central for supplementary material.

Acknowledgements

We thank T. Pritchett for technical assistance and P. Francisco for help on some of the auditory CS experiments. We thank G. Costa for illustrations and the Champalimaud Research Hardware Platform for technical support. We thank J. Fayad and M. Orger for advice on data analysis. We are grateful to the Carey lab and the members of the Champalimaud Neuroscience Program for helpful discussions throughout the project and in particular to H. Marques and J. Jacobs for comments on the manuscript. This work was supported by a Howard Hughes Medical Institute International Early Career Scientist Grant #55007413 (to MRC), Bial Foundation Bursary #74/14 (to DLP), fellowships from the Portuguese Fundação para a Ciência e a Tecnologia #BD77686/2011 (to CA) and #BPD109659/2015 (to DLP), and European Research Council Starting Grant #640093 (to MRC).

References

1. Vinck M, Batista-Brito R, Knoblich U, Cardin JA. Arousal and locomotion make distinct contributions to cortical activity patterns and visual encoding. Neuron. 2015; 86:740–754. [PubMed: 25892300]
2. Niell CM, Stryker MP. Modulation of visual responses by behavioral state in mouse visual cortex. Neuron. 2010; 65:472–479. [PubMed: 20188652]

3. Bennett C, Arroyo S, Hestrin S. Subthreshold mechanisms underlying state-dependent modulation of visual responses. Neuron. 2013; 80:350–357. [PubMed: 24139040]
4. Schneider DM, Nelson A, Mooney R. A synaptic and circuit basis for corollary discharge in the auditory cortex. Nature. 2014; 513:189–194. [PubMed: 25162524]
5. Zhou M, et al. Laminar-specific Scaling Down of Balanced Excitation and Inhibition in Auditory Cortex by Active Behavioral States. Nat Neurosci. 2014; 17:841–850. [PubMed: 24747575]
6. Williamson RS, Hancock KE, Shinn-Cunningham BG, Polley DB. Locomotion and task demands differentially modulate thalamic audiovisual processing during active search. Curr Biol. 2015; 25:1885–1891. [PubMed: 26119749]
7. Ayaz A, Saleem AB, Schölvinck ML, Carandini M. Locomotion Controls Spatial Integration in Mouse Visual Cortex. Curr Biol. 2013; 23:890–894. [PubMed: 23664971]
8. McGinley MJ, et al. Waking State: Rapid Variations Modulate Neural and Behavioral Responses. Neuron. 2015; 87:1143–1161. [PubMed: 26402600]
9. Ozden I, Dombeck DA, Hoogland TM, Tank DW, Wang SSH. Widespread State-Dependent Shifts in Cerebellar Activity in Locomoting Mice. PLoS One. 2012; 7:e42650. [PubMed: 22880068]
10. Powell K, Mathy A, Duguid I, Häusser M. Synaptic representation of locomotion in single cerebellar granule cells. Elife. 2015; 4:e07290.
11. Hoogland TM, De Gruijl JR, Witter L, Canto CB, De Zeeuw CI. Role of Synchronous Activation of Cerebellar Purkinje Cell Ensembles in Multi-joint Movement Control. Curr Biol. 2015; 25:1157–1165. [PubMed: 25843032]
12. Ghosh KK, et al. Miniaturized integration of a fluorescence microscope. Nat Methods. 2011; 8:871–878. [PubMed: 21909102]
13. Medina JF, Nores WL, Ohyama T, Mauk MD. Mechanisms of cerebellar learning suggested by eyelid conditioning. Curr Opin Neurobiol. 2000; 10:717–724. [PubMed: 11240280]
14. Gormezano I, Kehoe EJ, Marshall BS. Twenty years of classical conditioning research with the rabbit. Prog Psychobiol Physiol Psychol. 1983; 10:78.
15. Kim JJ, Thompson RE. Cerebellar circuits and synaptic mechanisms involved in classical eyeblink conditioning. Trends Neurosci. 1997; 20:177–181. [PubMed: 9106359]
16. De Zeeuw CI, Yeo CH. Time and tide in cerebellar memory formation. Curr Opin Neurobiol. 2005; 15:667–674. [PubMed: 16271462]
17. Carey MR. Synaptic mechanisms of sensorimotor learning in the cerebellum. Curr Opin Neurobiol. 2011; 21:609–615. [PubMed: 21767944]
18. McCormick DA, Thompson RF. Cerebellum: essential involvement in the classically conditioned eyelid response. Science (80-.). 1984; 223:296.
19. Steinmetz JE. Brain substrates of classical eyeblink conditioning: a highly localized but also distributed system. Behav Brain Res. 2000; 110:13–24. [PubMed: 10802300]
20. Gentet LJ, Avermann M, Matyas F, Staiger JF, Petersen CCH. Membrane Potential Dynamics of GABAergic Neurons in the Barrel Cortex of Behaving Mice. Neuron. 2010; 65:422–435. [PubMed: 20159454]
21. McGinley MJ, David SV, McCormick DA. Cortical membrane potential signature of optimal states for sensory signal detection. Neuron. 2015; 87:179–192. [PubMed: 26074005]
22. Reimer J, et al. Pupil fluctuations track fast switching of cortical states during quiet wakefulness. Neuron. 2014; 84:355–362. [PubMed: 25374359]
23. Reimer J, et al. Pupil fluctuations track rapid changes in adrenergic and cholinergic activity in cortex. Nat Commun. 2016; 7:13289. [PubMed: 27824036]
24. Joshi S, Li Y, Kalwani RM, Gold JI. Relationships between Pupil Diameter and Neuronal Activity in the Locus Coeruleus, Colliculi, and Cingulate Cortex. Neuron. 2016; 89:221–234. [PubMed: 26711118]
25. Kloosterman NA, et al. Pupil size tracks perceptual content and surprise. Eur J Neurosci. 2015; 41:1068–1078. [PubMed: 25754528]
26. Steinmetz JE, Rosen DJ, Chapman PF, Lavond DG, Thompson RF. Classical conditioning of the rabbit eyelid response with a mossy-fiber stimulation CS: I. Pontine nuclei and middle cerebellar peduncle stimulation. Behav Neurosci. 1986; 100:878–887. [PubMed: 3814342]

27. Hull C, Regehr WG. Identification of an inhibitory circuit that regulates cerebellar Golgi cell activity. Neuron. 2012; 73:149–158. [PubMed: 22243753]
28. Osborne LC, Lisberger SG, Bialek W. A sensory source for motor variation. Nature. 2005; 437:412–416. [PubMed: 16163357]
29. Gao Z, et al. Excitatory Cerebellar Nucleocortical Circuit Provides Internal Amplification during Associative Conditioning. Neuron. 2016; 89:645–57. [PubMed: 26844836]
30. Ishikawa T, Shimuta M, Häusser M. Multimodal sensory integration in single cerebellar granule cells in vivo. Elife. 2015; 4:e12916. [PubMed: 26714108]
31. Sawtell NB. Multimodal Integration in Granule Cells as a Basis for Associative Plasticity and Sensory Prediction in a Cerebellum-like Circuit. Neuron. 2010; 66:573–584. [PubMed: 20510861]
32. Huang C-C, et al. Convergence of pontine and proprioceptive streams onto multimodal cerebellar granule cells. Elife. 2013; 2:e00400. [PubMed: 23467508]
33. Jörntell H, Ekerot C-F. Properties of somatosensory synaptic integration in cerebellar granule cells in vivo. J Neurosci. 2006; 26:11786. [PubMed: 17093099]
34. Koekkoek SKE, Den Ouden WL, Perry G, Highstein SM, De Zeeuw CI. Monitoring Kinetic and Frequency-Domain Properties of Eyelid Responses in Mice With Magnetic Distance Measurement Technique. J Neurophysiol. 2002; 88:2124. [PubMed: 12364534]
35. Boele HJ, Koekkoek SKE, De Zeeuw CI. Cerebellar and extracerebellar involvement in mouse eyeblink conditioning: the ACDC model. Front Cell Neurosci. 2010; 3:19. [PubMed: 20126519]
36. Meijer JH, Robbers Y. Wheel running in the wild. Proceedings Biol Sci. 2014; 281 20140210.
37. Aston-Jones G, Cohen JD. An Integrative Theory of Locus Coeruleus-Norepinephrine Function: Adaptive Gain and Optimal Performance. Annu Rev Neurosci. 2005; 28:403–450. [PubMed: 16022602]
38. Carey MR, Regehr WG. Noradrenergic control of associative synaptic plasticity by selective modulation of instructive signals. Neuron. 2009; 62:112–122. [PubMed: 19376071]
39. Dieudonné S. Book review: serotonergic neuromodulation in the cerebellar cortex: cellular, synaptic, and molecular basis. Neurosci. 2001; 7:207–219.
40. Olson L, Fuxe K. On the projections from the locus coeruleus noradrenaline neurons: the cerebellar innervation. Brain Res. 1971; 28:165–171. [PubMed: 4104275]
41. Bloom FE, Hoffer BJ, Siggins GR. Studies on norepinephrine-containing afferents to Purkinje cells of rat cerebellum. I. Localization of the fibers and their synapses. Brain Res. 1971; 25:501–521. [PubMed: 5544323]
42. Paukert M, et al. Norepinephrine controls astroglial responsiveness to local circuit activity. Neuron. 2014; 82:1263–1270. [PubMed: 24945771]
43. Martins ARO, Froemke RC. Coordinated forms of noradrenergic plasticity in the locus coeruleus and primary auditory cortex. Nat Neurosci. 2015; 18:1483–1492. [PubMed: 26301326]
44. Ciocchi S, Passecker J, Malagon-Vina H, Mikus N, Klausberger T. Brain computation. Selective information routing by ventral hippocampal CA1 projection neurons. Science. 2015; 348:560–3. [PubMed: 25931556]
45. Jayaprakash N, et al. Optogenetic Interrogation of Functional Synapse Formation by Corticospinal Tract Axons in the Injured Spinal Cord. J Neurosci. 2016; 36:5877–5890. [PubMed: 27225775]
46. Tye KM, et al. Amygdala circuitry mediating reversible and bidirectional control of anxiety. Nature. 2011; 471:358–362. [PubMed: 21389985]
47. Bengtsson F, Jörntell H. Sensory transmission in cerebellar granule cells relies on similarly coded mossy fiber inputs. Proc Natl Acad Sci. 2009; 106:2389–2394. [PubMed: 19164536]
48. ten Brinke MM, et al. Evolving Models of Pavlovian Conditioning: Cerebellar Cortical Dynamics in Awake Behaving Mice. Cell Rep. 2015; 13:1977–1988. [PubMed: 26655909]
49. Chabrol FP, Arenz A, Wiechert MT, Margrie TW, DiGregorio DA. Synaptic diversity enables temporal coding of coincident multisensory inputs in single neurons. Nat Neurosci. 2015; 18:718–727. [PubMed: 25821914]
50. Edgley SA, Lidierth M. The discharges of cerebellar Golgi cells during locomotion in the cat. J Physiol. 1987; 392:315–32. [PubMed: 3446782]

51. Arenkiel BR, et al. In Vivo Light-Induced Activation of Neural Circuitry in Transgenic Mice Expressing Channelrhodopsin-2. Neuron. 2007; 54:205–218. [PubMed: 17442243]
52. Barski JJ, Dethleffsen K, Meyer M. Cre recombinase expression in cerebellar Purkinje cells. Genesis. 2000; 28:93–8. [PubMed: 11105049]
53. Madisen L, et al. A toolbox of Cre-dependent optogenetic transgenic mice for light-induced activation and silencing. Nat Neurosci. 2012; 15:793–802. [PubMed: 22446880]
54. Fünfschilling U, Reichardt LF. Cre-Mediated Recombination in Rhombic Lip Derivatives. Genesis. 2002; 33:160–169. [PubMed: 12203913]
55. Carey MR, et al. Presynaptic CB1 Receptors Regulate Synaptic Plasticity at Cerebellar Parallel Fiber Synapses. J Neurophysiol. 2011; 105:958–963. [PubMed: 21084685]
56. Heiney SA, Kim J, Augustine GJ, Medina JF. Precise Control of Movement Kinematics by Optogenetic Inhibition of Purkinje Cell Activity. J Neurosci. 2014; 34:2321–2330. [PubMed: 24501371]
57. Mostofi A, Holtzman T, Grout AS, Yeo CH, Edgley SA. Electrophysiological Localization of Eyeblink-Related Microzones in Rabbit Cerebellar Cortex. J Neurosci. 2010; 30:8920–8934. [PubMed: 20592214]
58. Van Der Giessen RS, et al. Role of Olivary Electrical Coupling in Cerebellar Motor Learning. Neuron. 2008; 58:599–612. [PubMed: 18498740]
59. Steinmetz AB, Freeman JH. Localization of the Cerebellar Cortical Zone Mediating Acquisition of Eyeblink Conditioning in Rats. Neurobiol Learn Mem. 2014; 114:148–154. [PubMed: 24931828]
60. Yeo CH, Hardiman MJ, Glickstein M. Classical conditioning of the nictitating membrane response of the rabbit I. Lesions of the cerebellar nuclei. Exp Brain Res. 1985; 60:87–98. [PubMed: 4043285]
61. Ohmae S, Medina JF. Climbing fibers encode a temporal-difference prediction error during cerebellar learning in mice. Nat Neurosci. 2015; 18:1798–1803. [PubMed: 26551541]
62. Chettih SN, McDougle SD, Ruffolo LI, Medina JF. Adaptive Timing of Motor Output in the Mouse: The Role of Movement Oscillations in Eyelid Conditioning. Front Integr Neurosci. 2011; 5:72. [PubMed: 22144951]
63. Heiney SA, Wohl MP, Chettih SN, Ruffolo LI, Medina JF. Cerebellar-Dependent Expression of Motor Learning during Eyeblink Conditioning in Head-Fixed Mice. J Neurosci. 2014; 34:14845–14853. [PubMed: 25378152]
64. Machado AS, Darmohray DM, Fayad J, Marques HG, Carey MR. A quantitative framework for whole-body coordination reveals specific deficits in freely walking ataxic mice. Elife. 2015; 4
65. Lee KH, et al. Circuit Mechanisms Underlying Motor Memory Formation in the Cerebellum. Neuron. 2015; 86:529–540. [PubMed: 25843404]
66. Siegle JH, Hale GJ, Newman JP, Voigts J. Neural ensemble communities: Open-source approaches to hardware for large-scale electrophysiology. Curr Opin Neurobiol. 2015; 32:53–59. [PubMed: 25528614]
67. Lopes G, et al. Bonsai: an event-based framework for processing and controlling data streams. Front Neuroinform. 2015; 9:7. [PubMed: 25904861]
68. Van Dijck G, et al. Probabilistic Identification of Cerebellar Cortical Neurones across Species. PLoS One. 2013; 8:e57669. [PubMed: 23469215]

Europe PMC Funders Author Manuscripts

Europe PMC Funders Author Manuscripts

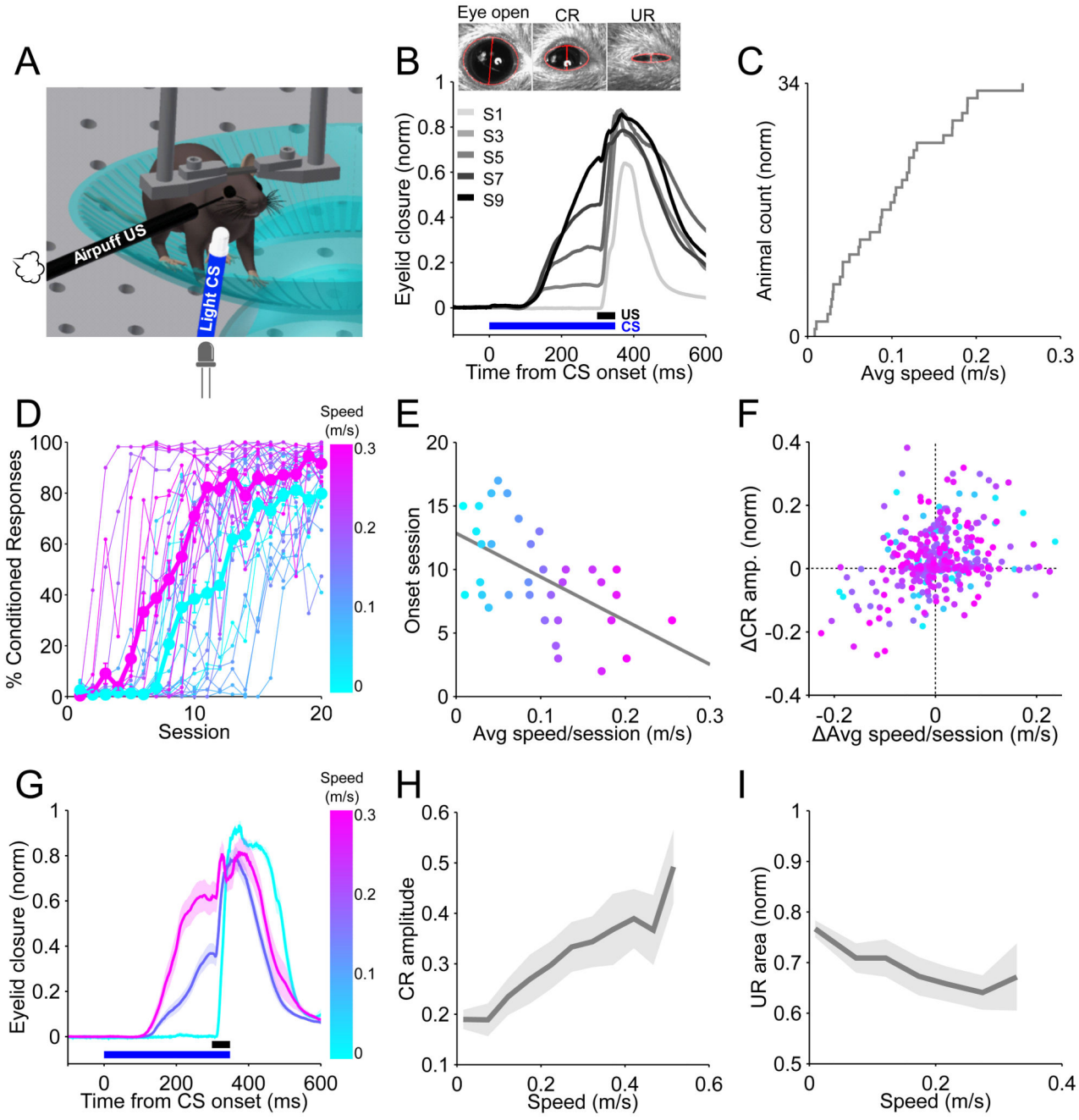

Fig. 1. Eyeblink conditioning performance correlates with locomotor activity across mice, sessions, and trials

A. Setup schematic for eyeblink conditioning in head-fixed mice on a running wheel, illustrating a white LED as the CS and an air puff US. **B**. Average eyelid closure for a representative animal across 9 learning sessions (S1-S9). Each trace represents the average of 100 paired trials from a single session. Example video frames (acquired at 900 fps under infrared light) illustrate automated extraction of eyelid movement amplitude. **C**. Cumulative histogram of locomotor activity of all animals (N=34) trained with a light CS, calculated by

averaging the average speed of each session. **D**. Learning curves for all animals represented in (C), color-coded for their average speed. Averages of the 20% fastest and slowest mice are superimposed in magenta and cyan, respectively. **E**. Onset session of learning for each animal, plotted against the animals' average walking speed. Onset session was defined as the session in which the average CR amplitude exceeded 0.1. Each dot represents an animal. The line is a linear fit (N=34, slope = -34.4, ***p = 0.00057). See also Supp. Fig. 1. **F**. Session-to-session changes in average CR amplitude (y-axis) are plotted as a function of session-to-session changes in locomotor activity (x-axis), for all learning sessions, color-coded for the average speed of each session. There was a significant positive relationship (one-way ANOVA on linear mixed effects model (LME), n=646 sessions, N=34 animals, F(1,155) = 24.271, ***p = 2.127e-6) between changes in walking speed and changes in CR amplitude. **G**. Average of trials from session 6 of one representative animal, divided into 3 speed intervals (<0.1m/s (18 trials); 0.2-0.25m/s (20 trials); >0.35m/s (16 trials)) and color-coded accordingly. Shadows represent SEM. **H**. Trial-to-trial correlation between CR amplitude and walking speed. CR amplitudes for all trials from the session in which each individual animal crossed a threshold of 50% CR plus the following session are plotted. Line is average across animals; shadow indicates SEM. There was a linear positive relationship (one-way ANOVA on LME, n=7,480 trials, N=34 animals, F(1,180.29) = 83.023, ***p = 1.55e-16) between running speed and conditioned response amplitude. **I**. Correlation between unconditioned response (UR) magnitude and walking speed from trial-to-trial. The normalized area under the UR in response to the air puff is plotted for Session 1, before emergence of conditioned responses. Line is average across animals; shadow indicates SEM. There was a linear negative relationship (one-way ANOVA on LME, n=3,332 trials, N=34 animals, F(1,91.898) = 27.366, ***p 1.05e-6) between running speed and UR amplitudes.

Europe PMC Funders Author Manuscripts

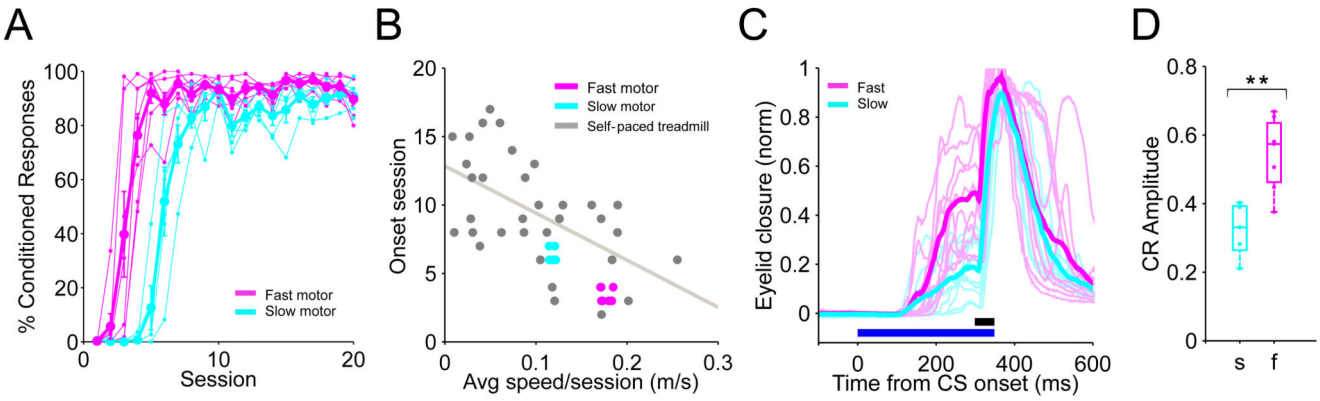

Fig. 2. Speed-dependent modulation of eyeblink conditioning on a motorized treadmill

A. Individual learning curves with superimposed averages of two groups of mice, running on either a faster (magenta, 0.18m/s, N=7) or slower (cyan, 0.12m/s, N=5) motorized treadmill. **B**. Quantification of learning onset session for each animal. Fast (magenta) and slow (cyan) motorized data are superimposed on the self-paced treadmill data from Fig. 1E (gray). The difference in learning onset between the fast and slow group was significant (average session 3.4 vs. 6.4, respectively, ***p = 2.79e-6, Student's two-sided t-test). **C**. Eyelid traces of individual trials for individual representative animals on the fast (magenta) vs. slow (cyan) motorized treadmills at learning session 7. The traces for every 10th trial are shown. **D**. Median CR amplitudes from S7 for animals (dots) running at the slow (s, cyan, N=5) or fast (f, magenta, N=7) motorized speed (fast vs. slow, **p = 0.003, Student's two-sided t-test). Box indicates median and 25^{th}-75^{th} percentiles, whiskers extend to the most extreme data points. Significance: *p < 0.05, **p < 0.01 and ***p < 0.001.

Europe PMC Funders Author Manuscripts

Europe PMC Funders Author Manuscripts

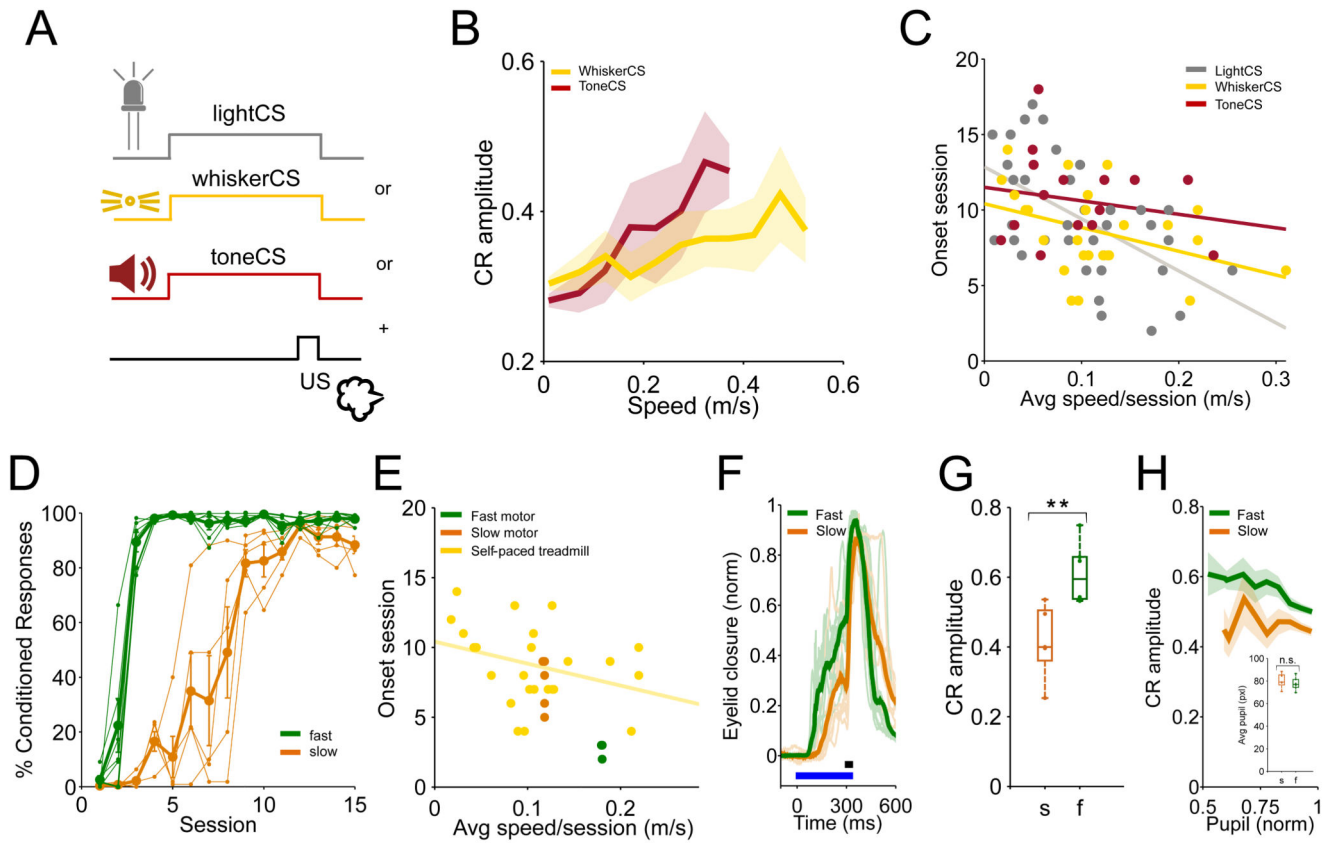

Fig. 3. Modulation of CR acquisition and amplitude are CS-independent and dissociable from effects of arousal

A. Schematic for experiments using conditioned stimuli of different sensory modalities: light CS in gray, tactile (whisker) CS in orange and auditory (tone) CS in red; each was paired with an airpuff US. **B**. Trial-to-trial correlation between CR amplitude and walking speed for all trials with CRs from all training sessions using a whisker (in yellow) or a tone (in red) CS. Line is average across animals; shadow indicates SEM. There was a significant positive relationship for both whisker (one-way ANOVA on LME, n=15490 trials, N=25 animals, F(1,159.8) = 11.499, ***p = 0.0009) and tone (n=9771 trials, N=16 animals, F(1,82.5) = 32.255, ***p = 1.968e-7). **C**. Onset learning session for animals from all three CS modalities, color-coded as in (A), plotted against the average walking speed of each animal on the self-paced treadmill. The lines are linear fits (visual CS from Fig. 1E; whisker CS: N=25 animals, slope=-15.7; p=0.052; tone CS: N=16 animals, slope=-8.9; p=0.49). **D**. Individual whisker CS learning curves with averages superimposed of two groups of mice running on either a faster (green, 0.18m/s, N=6) or slower (orange, 0.12m/s, N=5) motorized treadmill. **E**. Quantification of learning onset session for each animal from (D). Fast (green) and slow (orange) motorized data are superimposed on the self-paced treadmill (yellow). The difference in onset learning between the fast and slow group was significant (***p = 1.92e-4, Student's two-sided t-test). **F**. Eyelid traces of individual trials for a representative animal on the fast (green) vs. slow (orange) motorized treadmill at S10. **G**. Quantification of CR amplitudes from S10 for animals (dots) running either at the slow (orange) or fast

(green) motorized speed. The slow and fast groups were significantly different (**p = 0.0094, Student's two-sided t-test). Box indicates median and 25^{th}-75^{th} percentiles, whiskers extend to the most extreme data points. **H**. Relationship between CR amplitude and pupil size for all CR trials from training sessions using a whisker CS on the fast (one-way ANOVA on LME, n=8249 trials, N=6 animals, F(1,102) = 10.35, **p = 0.0017) versus slow (one-way ANOVA on LME, n=4194 trials, N=5 animals, F(1,38) = 2.929, p = 0.095) motorized treadmill. Line is average across animals; shadow indicates SEM. Inset: Median pupil size (pixels) for both speeds (difference not significant, p = 0.5109, Student's two-sided t-test). Box indicates median and 25^{th}-75^{th} percentiles, whiskers extend to the most extreme data points. Significance: *p < 0.05, **p < 0.01 and ***p < 0.001.

Europe PMC Funders Author Manuscripts

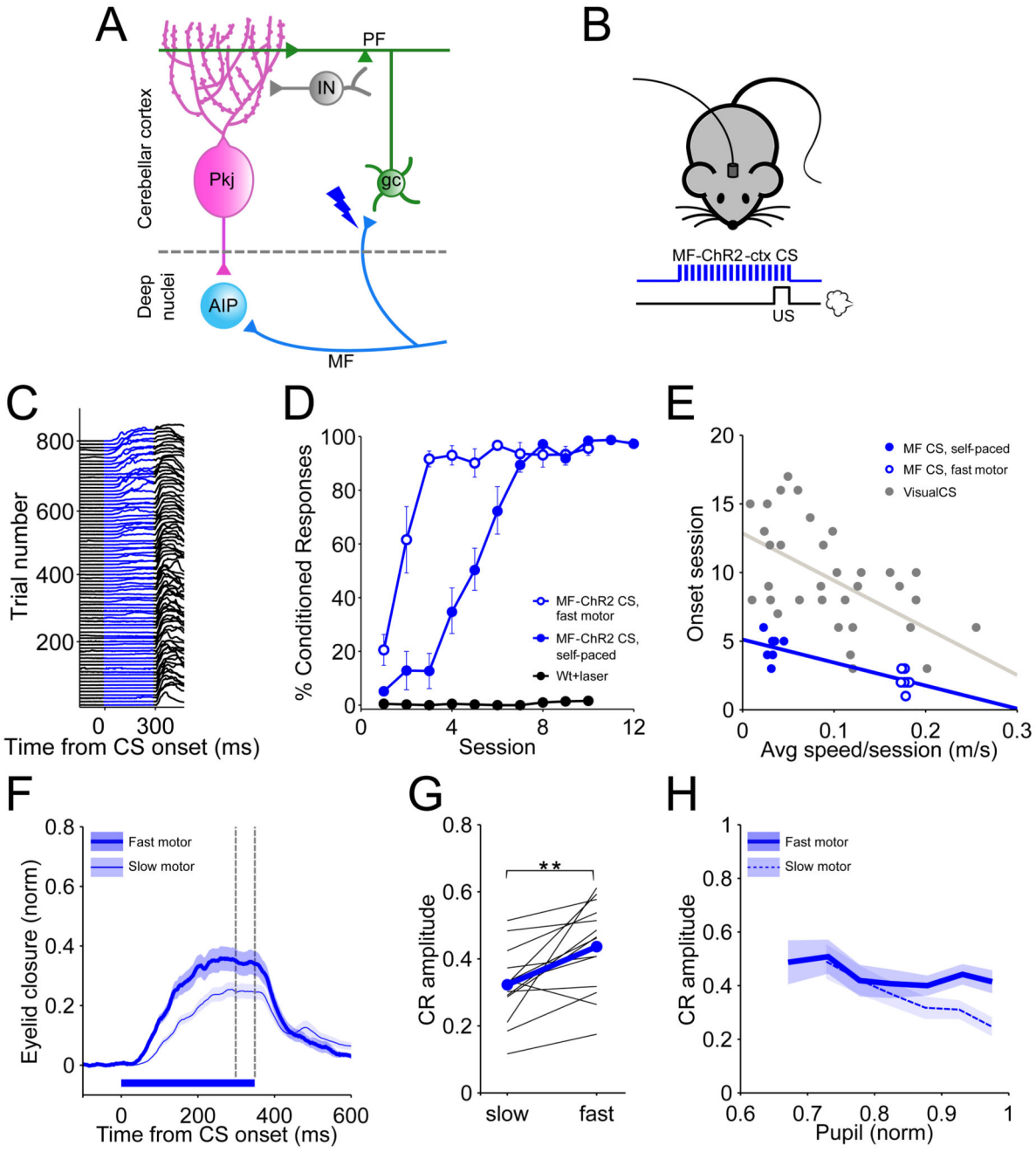

Fig. 4. Conditioned responses acquired with optogenetic stimulation of cerebellar mossy fibers in the cerebellar cortex are positively modulated by locomotor activity

A. Cerebellar circuit diagram with a blue lightning bolt representing the site of laser stimulation: mossy fiber terminals in eyelid-related cerebellar cortex. **B.** Schematic of eyelid conditioning protocol using MF-ChR2-ctx optogenetic stimulation as a replacement for the CS. Animals implanted with optical fibers in an eyelid-related region of cerebellar cortex were trained to a sub-threshold (i.e. not eliciting eye movement) laser stimulation of mossy fibers (473nm light pulses at 100Hz for 350ms) paired with an airpuff to the eye as US. **C.**

Europe PMC Funders Author Manuscripts

Representative individual trials for one mouse trained with a MF-ChR2-ctx CS and airpuff US, during the first eight sessions. The eyelid trace for every 9th trial from eight sessions is plotted. **D.** Average %CR learning curves to MF-ChR2-ctx CS's for animals walking on a self-paced treadmill (filled circles, N=7), and animals running at a fast fixed speed (0.18m/s, N=7) on the motorized treadmill (open circles). To control for the possibility that the mice could see the laser, which could inadvertently act as a visual CS, wildtype controls (not expressing ChR2) were implanted with optical fibers and underwent the same training protocol (black circles, N=4). Error bars indicate SEM. **E.** Learning onset session for the animals in D are superimposed on the self-paced treadmill data from mice trained to a visual CS (gray). The blue line is a linear fit (onset value: slope = -16.8, **p = 0.00015). **F G H** After learning reached a plateau, both groups were tested for the expression of CRs in test sessions at two fixed speeds on the motorized treadmill: slow (0.06m/s) and fast (0.18m/s). (**F**) Average of CS-only trials (n=50 trials) from the slow (dashed line) and fast (solid line) blocks of trials, for one representative animal. Shadows indicate SEM. Vertical dashed lines represent the time that the US would have been expected on CS+US trials. (**G**) Average CR amplitude of responses from each animal (N=15) walking at slow (0.06m/s) *vs* fast (0.18m/s) pace on the motorized treadmill. The average from all animals is superimposed (in blue, **p = 0.0017, Student's two-sided paired t-test). (**H**) Relationship between CR amplitude and pupil size for all CR trials from test sessions with an optogenetic CS on the fast (solid line, one-way ANOVA on LME, n=1501 trials, N=15 animals, $F(1,55.3) = 0.845$, $p = 0.36192$) vs. slow (dashed line, one-way ANOVA on LME, n=1501 trials, N=15 animals, $F(1,11.9) = 59.5$, *p = 0.001) motorized treadmill. Line is average across animals; shadow indicates SEM. Significance: *p < 0.05, **p < 0.01 and ***p < 0.001.

Europe PMC Funders Author Manuscripts

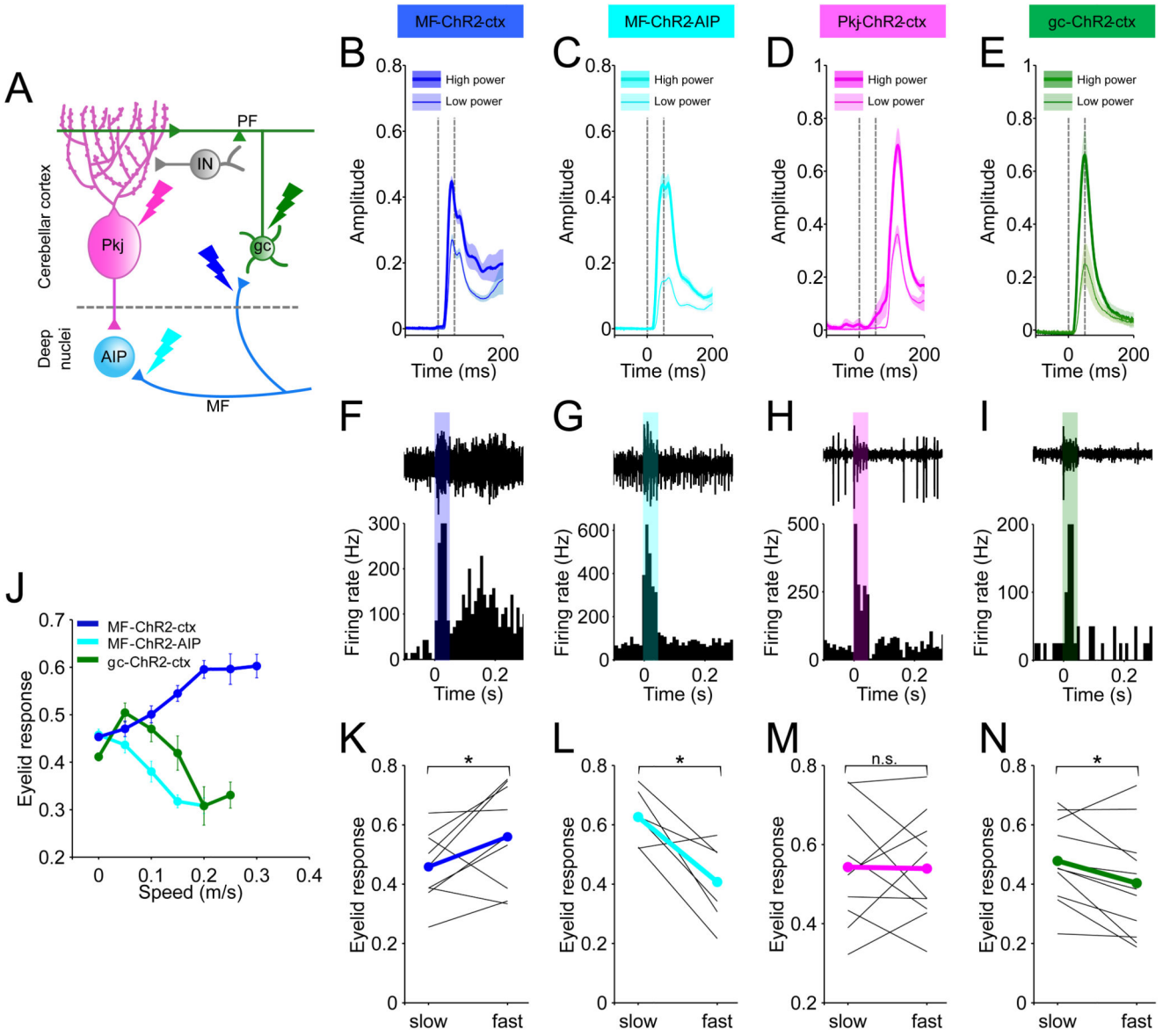

Fig. 5. Eyelid closures evoked by optogenetic MF stimulation in the cerebellar cortex are positively modulated by locomotion

A. Schematic of the cerebellar circuit including some of the major cell types in the cerebellar cortex and deep nuclei. Lightning bolts represent the different targets of laser stimulation: mossy fibers (MF) terminals in the cerebellar cortex (blue), MF terminals in the deep nuclei (cyan), granule cells (gc, green) and Purkinje cells (Pkj, pink). IN, interneuron; PF, parallel fiber; AIP, anterior interpositus. **B-E.** Eyelid movements from a representative animal from each mouse line in response to supra-threshold laser stimulation (473nm light pulses at 100Hz for 50ms) at two different intensities. Vertical dashed lines represent the stimulus duration; average (of 10-20 trials each) represented by the thick line; shadows indicate SEM. Laser pulse duration is indicated by the vertical dashed lines. **B,C.** An optical fiber was placed in an identified eyelid-related region of cerebellar cortex (**B**, blue) or AIP

Europe PMC Funders Author Manuscripts

(**C**, cyan) of Thy1-ChR2-YFP mice that express ChR2 in cerebellar mossy fibers. **D,E.** An optical fiber was placed in the same eyelid region of cerebellar cortex in mice that express ChR2 in Purkinje cells (L7cre-ChR2-YFP, **D**, pink) or cerebellar granule cells (Gabra6cre-ChR2-YFP, **E**, green). **F-I.** *In vivo* electrophysiological responses to 50 ms laser stimulation in awake mice for the lines depicted in (**B-E**). Example extracellular traces are shown above the peri-stimulus time histograms and laser pulse durations are indicated by the shadows of corresponding colors. **F**. *In vivo* recordings from units in cerebellar cortex in response to MF-ChR2-ctx stimulation. **G**. *In vivo* recordings from units in cerebellar nuclei in response to MF-ChR2-AIP stimulation. **H.** *In vivo* recordings from units in cerebellar cortex in response to Pkj-ChR2-ctx stimulation. **I.** *In vivo* recordings from units in cerebellar cortex in response to gc-ChR2-ctx stimulation. **J.** Correlation between laser-driven eyelid responses and walking speed on the self-paced treadmill from trial-to-trial, for MF-ChR2-ctx mice (blue, n=1072 trials, N=8 animals; one-way ANOVA on LME, $F(1,1068.8) = 5.01$, $^{*}p = 0.025$); MF-ChR2-AIP mice (cyan, n=502 trials, N=5 animals; $F(1,501.8) = 4.02$, $^{*}p = 0.04$); and gc-ChR2-ctx mice (green, n=943 trials, N=11 animals; $F(1,939.5) = 30.68$, $^{***}p = 3.95e-08$). Lines represent trial-wise averages from all animals and error bars indicate SEM. **K-N.** Average amplitude of laser-elicited eye closures from animals walking at slow (0.06m/s) or fast (0.18m/s) pace, as set by the motorized treadmill. Each animal was tested for the two speeds within one session, using the same stimulation protocol and laser intensity. The average from all animals is superimposed. **K.** Laser-elicited blink in MF-ChR2-ctx mice (N=7; $^{*}p = 0.0298$, Student's paired t-test); **L.** laser-elicited blink in MF-ChR2-AIP mice (N=6; $^{*}p = 0.0197$, Student's two-sided paired t-test); **M.** Laser-elicited blink in Pkj-ChR2-ctx mice (N=10; $p = 0.9361$, Student's two-sided paired t-test); **N.** Laser-elicited blink in gc-ChR2-ctx mice (N=11; $^{*}p = 0.03$, Student's two-sided paired t-test). Significance: $^{*}p < 0.05$, $^{**}p < 0.01$ and $^{***}p < 0.001$.

Europe PMC Funders Author Manuscripts

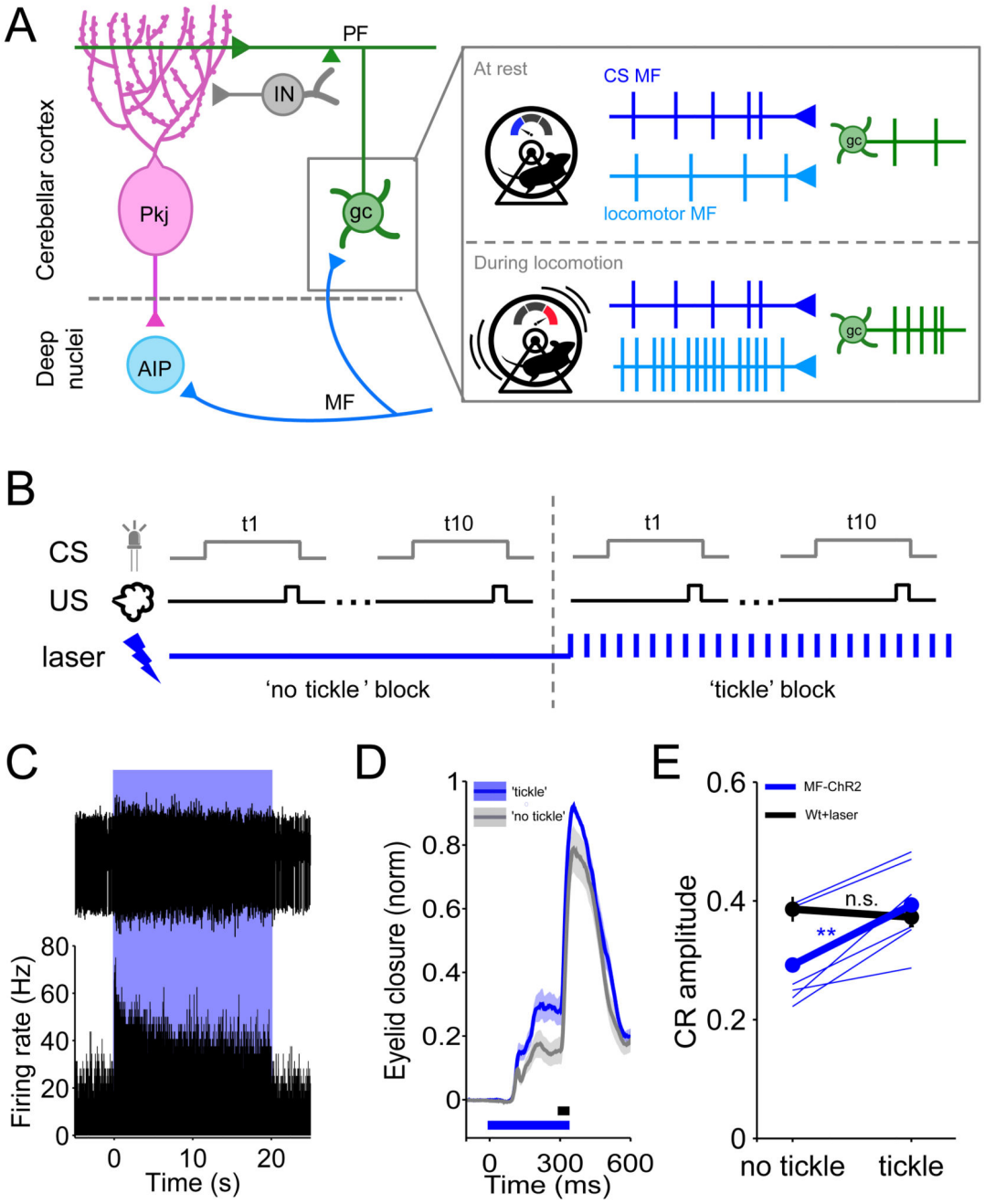

Fig. 6. Low-level background mossy fiber stimulation is sufficient to enhance conditioned response amplitude

A. Schematic illustrating proposed mechanism for CR modulation by locomotor activity. Distinct mossy fiber terminals (depicted here as one CS mossy fiber and one 'locomotor' mossy fiber) converge onto individual granule cells. Summation of multiple mossy fiber inputs is required for postsynaptic granule cell firing. Enhanced mossy fiber tone during locomotion (bottom) therefore leads to enhanced granule cell CS responses relative to when the mouse is stationary (top). **B.** Experimental design: After training MF-ChR2-YFP mice

implanted with optical fibers in an eyelid-related region of cerebellar cortex, using a visual CS and an airpuff US, trials were presented in alternating blocks of 10 trials, either without stimulation (‘no tickle’ block), or with extremely low intensity 50 Hz, 2ms pulses, background optogenetic stimulation of mossy fibers in the cerebellar cortex (‘tickle’ block). Motorized treadmill speed was fixed (0.12m/s) throughout the experiment. **C.** *In vivo* electrophysiological responses to 20 s laser stimulation (50 Hz, 2ms pulses) delivered through an optical fiber implanted in the eyelid region of cerebellar cortex in an awake MF-ChR2-YFP mouse. An example extracellular trace is shown above the peri-stimulus time histogram and laser pulse duration is indicated by the blue shadow. **D.** Average of eyelid traces from ‘tickle’ (blue) and ‘no tickle’ (gray) blocks (21 trials in each average), for a representative animal. Shadows indicate SEM. **E.** Comparison of CR amplitudes with (left) vs without (right) laser stimulation, in MF-ChR2 mice (blue, N=6, **p = 0.0031, Student’s two-sided paired t-test) and wildtype controls (not expressing ChR2, black, N=4, p = 0.6014, Student’s two-sided paired t-test). Thin lines represent individual animals, thick lines are averages across animals. Error bars represent SEM. Significance: *p < 0.05, **p < 0.01 and ***p < 0.001.

Europe PMC Funders Author Manuscripts